Title: **Predicting Processing Induced Residual-Stresses in Carbon Fiber–Thermoplastic Micro-Composites**

Authors (names are for example only): Nithin K. Parambil[1*]
Branndon R. Chen[1, 2]
Joseph M. Deitzel[1]
John W. Gillespie Jr.[1,2,3,4,5]
Loan T. Vo[6]
Peter Sarosi[6]

(FIRST PAGE OF ARTICLE)

ABSTRACT

A computational model of residual stress is developed for AS4/polypropylene composites and implemented via user material subroutine (UMAT) in ABAQUS. The main factors included in the model are the cooling-rate dependent crystallinity, temperature-dependent elastic modulus, and temperature-dependent coefficient of thermal expansion (CTE) of the matrix, and the temperature-independent transversely isotropic properties of the carbon fiber. Numerical results are generated for the case of a single fiber embedded in a thin film of polypropylene sample to replicate the process history and test configuration. During single fiber composite processing, a precalculated weight (tensile preload) is applied at the fiber ends to eliminate buckling/waviness of the carbon fiber induced by matrix shrinkage in the axial direction of the fiber. Experiments and Finite element (FE) analysis have been conducted with different preloads (1g, 4g, and 8g) at 25˚C. Micro-Raman spectroscopy is utilized to validate the residual strain with different preloads at the bulk. The measured strain values show a good correlation with the predicted residual strain for various preload conditions.

[1]Center for Composite Materials, University of Delaware. Newark, DE 19716, USA
[2]Department of Materials Science and Engineering, University of Delaware. Newark, DE 19716, USA
[3]Department of Mechanical Engineering, University of Delaware. Newark, DE 19716, USA
[4]Department of Civil and Environmental Engineering, University of Delaware. Newark, DE 19716, USA
[5]Department of Computer and Electrical Engineering, University of Delaware. Newark, DE 19716, USA
[6]ExxonMobil Research and Engineering Company, Annandale, NJ 08801, USA

INTRODUCTION

Manufacturing of thermoplastic matrices composites over thermoset matrices has increased in the last decades due to their high throughput. Thermoplastic composites (TPCs) can be processed in several minutes compared to a much more time-consuming cure cycle of thermoset composites. Additionally, thermoplastics are well known for their toughness, weldability, chemical resistance, recyclability, etc. However, thermal residual stress forms after processing at relatively high process temperature (150-250°C) and subsequent cooling to service temperature [1]. Residual stresses arise due to a mismatch in the coefficient of thermal expansion (CTE) of the matrix compared with the CTE of the fibers. Also, the inhomogeneous nature of fiber-reinforced polymers causes residual stresses. Residual stress can have significant effects on the dimensional stability/warpage and assembly tolerance and can contribute to the evolution of microstructural damage due to static and fatigue loading [1].

Rapid consolidation during the manufacturing of TPCs can result in through-thickness temperature gradients and non-uniform cooling-rate histories. In semicrystalline TPCs, complex cooling-rate histories influence the degree of crystallinity, which in turn influences the mechanical properties such as stiffness, modulus and fracture toughness, etc. [2] [3]. To accurately predict residual stresses, it is important to study the matrix cooling-rate dependent crystallization kinetics. The study of crystallization kinetics which is directly related to cooling rate is very important to measure residual stress. A material agnostic computational model was developed with detailed experimental inputs to predict the thermal residual stress developed in the TPCs. In this present study, AS4 carbon fiber and polypropylene matrix-based TPCs are the constituent materials of interest. Polypropylene's cooling-rate-dependent crystallinity, temperature-dependent elastic modulus, and temperature-dependent coefficient of thermal expansion (CTE), and CTE mismatch of matrix and carbon fiber are measured and modeled to predict the residual stress as a function of process history. ExxonMobil polypropylene blended with 10% ExxonMobil PO MAPP adhesion promoter and unsized Hexcel AS4 carbon fibers-based TPCs are used in this study. The proposed model can be used for more complex geometries like fiber pullout tests (micro-level) [4], composite laminae/laminates (meso/macro level), and structures.

RESIN THERMAL AND MECHANICAL PROPERTIES CHARACTERIZATION

NON-ISOTHERMAL CRYSTALLIZATION KINETICS OF ISOTACTIC POLYPROPYLENE (IPP)

Polypropylene is a semi-crystalline polymer that forms crystalline structures when cooled from melt under isothermal/non-isothermal conditions. The cooling rate affects the crystallization behavior of the polypropylene, and thus the resulting microstructure which in turn has a significant effect on the ultimate properties of the matrix and composite material. The constitutive model must accurately predict mechanical performance for a range of processing-induced crystallinities since the

specimen preparation for different purposes (for example pullout specimen/test for interface properties, resin characterization samples, etc.) have different cooling rate. Monitoring sample processing temperature allows us to predict crystallization and verify with differential scanning calorimetry (DSC).

A literature review was conducted to develop a computational model to predict crystallinity at different cooling rates. Different published mathematical models for the non-isothermal crystallization kinetics of iPP are available in the literature [5] [6] [7] [8] [9]. A proposed model by Hammami et al. represented a more accurate model compared to others were reported in [10]. The parameters for the crystallization model were determined by correlating and fitting the model with the experimental cooling rate studies. A non-isothermal crystallization model has been generated from the measurement of the crystallization behavior at different cooling rates. These parameters have been used to predict the processing induced crystallinity of the pullout samples and resin characterization samples as shown in Figure 1.

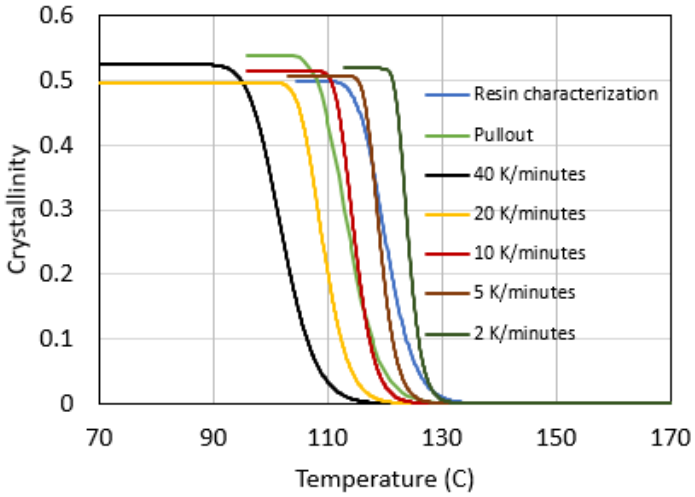

Figure 1. Crystallization prediction at different cooling rates from 2 – 40 K/minutes, singe fiber thin film sample, and resin characterization sample.

Onset and end temperature of crystallinity decrease with a cooling rate increase. The end temperature can be considered as a stress-free temperature for the residual stress calculation [11] [12] [13] [14] [15]. This generates a prediction of stress-free temperature as a function of cooling rate, shown in Figure 2. Crystallinity at the termination of the crystallization process is almost 50% for cooling rate range from 2-40 K/minute. With this information, it is possible to predict the composite residual stresses where the cooling rate may induce local variations.

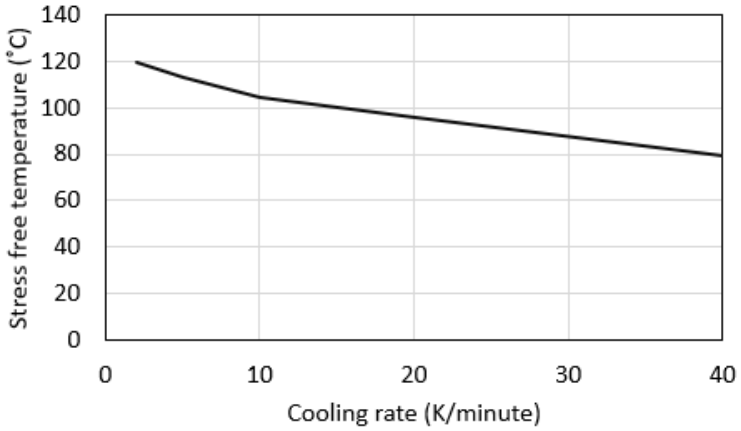

Figure 2. Stress-free temperature vs cooling rate.

RESIN CHARACTERIZATION AT DIFFERENT STRAIN RATES AND TEMPERATURES

The stress-free temperature at different cooling rates has been shown in Figure 2. This can be used as a reference for resin characterization at different temperatures. An initial computational study has been performed for the pullout/model composites to identify the local strain rates (1e-3 s^{-1} – 1e-1 s^{-1}) around the fiber/matrix interface for a particular range of applied far-field strain rates. The stress-strain responses of ExxonMobil PP were developed using quasi-static compression test on standard cylindrical specimen at different strain rates (1e-3 s^{-1}, 1e-2 s^{-1} and 1e-1 s^{-1}) and temperatures (120˚C, 60 ˚C, 25 ˚C, 0 ˚C, -30 ˚C and -40 ˚C). Modulus and yield stress were significantly affected by strain rates and temperatures as shown in Figure 3 and Figure 4. Incorporating these temperatures and rate-dependent factors in the model will provide a more accurate resin behavior than the simple analytical cases.

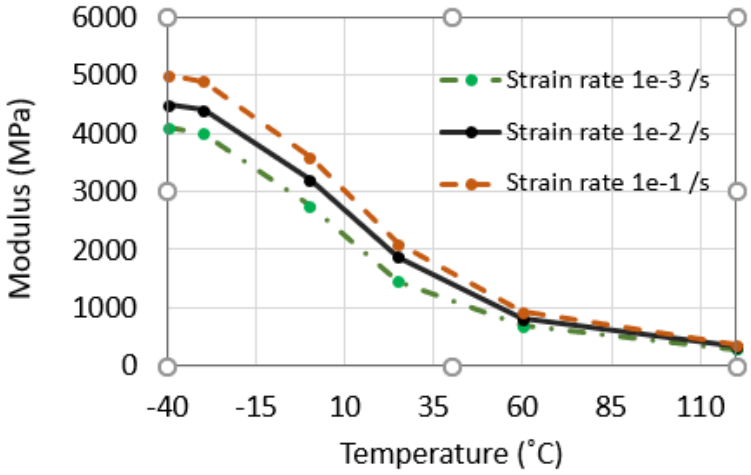

Figure 3. Modulus at different strain rates and temperatures.

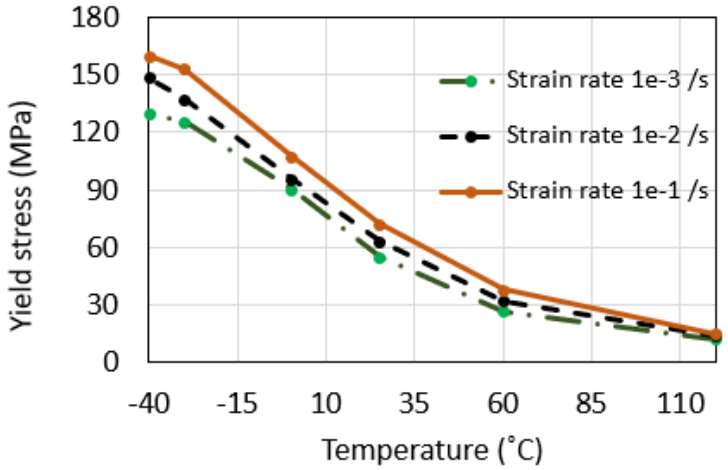

Figure 4. Yield stress at different strain rates and temperatures.

CALCULATION OF CTE USING THERMOMECHANICAL ANALYSIS (TMA)

The next step was to measure the CTE as a function of temperatures. TMA was used to measure the dimensional changes of a material as a function of temperature. CTE is the slope of dL/dL_0 vs temperature curve. Figure 5 shows the dL/dL_0 vs temperature. The fitted bi-linear curve represents the CTE above T_g and below T_g (CTE = 0.0002 /˚C above T_g and CTE = 0.00007 /˚C below Tg).

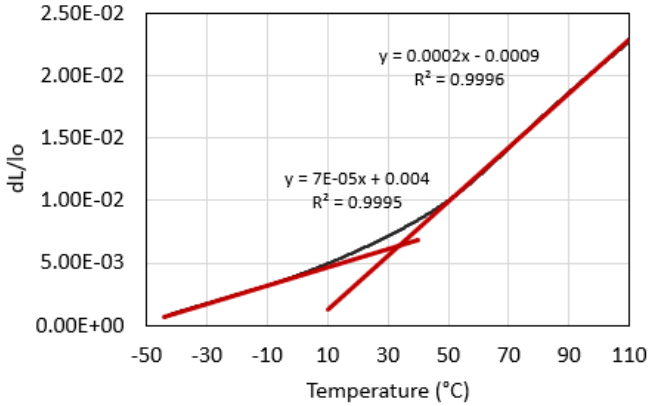

Figure 5. CTE calculation at different temperature

POLYPROPYLENE CONSTITUTIVE MODEL

We have developed a UMAT in ABAQUS for constitutive properties for PP, which incorporates the polypropylenes cooling-rate dependent crystallinity, temperature-dependent elastic modulus, and temperature-dependent coefficient of thermal expansion (CTE). The mathematical 3D Constitutive equation is shown in Eq 6. The Jacobian matrix of the constitutive model in Abaqus is shown in Eq 7.

$$\sigma_{ij} = C_{ijkl}\varepsilon_{ij} - C_{ijkl}\delta_{ij}\alpha\Delta T \quad (6)$$

where σ is stress tensor, ε is strain tensor, C – Stiffness matrix (function of temperature) α is the Coefficient of thermal expansion (function of temperature) and T is temperature.

$$J = \frac{\partial \Delta\sigma}{\partial \Delta\varepsilon} \quad (7)$$

where J is Jacobian matrix in ABAQUS

$$\sigma^{new} = \sigma^{old} + \Delta\sigma \quad (8)$$

$$\Delta\sigma = J\Delta\varepsilon \quad (9)$$

The resulting resin constitutive equation can serve as inputs to both the residual stress prediction and fiber pullout FE models. Accurate prediction of residual stress is only possible by matching the exact experimental procedures. The next sections explain the experimental procedures to measure the residual stresses and correlate/validate with this predictive capability at the single fiber level.

PREDICTION AND VALIDATION OF MICRO-COMPOSITE RESIDUAL STRESS

Using the FE model with implemented UMAT, we can predict residual stress induced by factors such as CTE mismatch between the resin and fiber, cooling rate dependent crystallinity, and applied mechanical load. The specimens' complete strain history must be accounted for (including from processing through testing) before any accurate predictions are made. Using the simple case of a single fiber fragmentation test (SFFT) specimen, we validate the predicted residual strain and compare it with a matching experimental condition. Varying fiber pretension (preload) is applied during and through sample processing to change the room temperature/cooled strain state. As pretension increases, the compressive fiber strain in the SFFT specimen reduces toward zero.

SINGLE FIBER SAMPLE PREPARATION

SFFT samples need to be optically transparent and uniform in thickness to match the FE model geometry and observe using the Micro-Raman technique. This was achieved by hot-pressing thin, 100μm films out of the polypropylene pellets. The as-received polypropylene pellets were pressed between two precision ground aluminum plates lined with Kapton films. The aluminum plate stack was hot-pressed in a Carver press with 6x6 at 220°C, a slight pressure of 1000lbs was applied to achieve the desired thickness with the shims. The sample was then forced air-cooled to room temperature at an approximate rate of -10°C/min.

Single AS4 fibers were separated and tabbed with Kapton. The prepared PP sheets were cut into two 2.5x5 in rectangles. One layer of Kapton film was placed on the aluminum platen, then the PP film. Fibers were laid across, then the second PP film was placed on top sandwiching the fibers. Kapton film shims were placed around the PP/fiber stack to minimize resin flow, careful attention was paid to prevent the fibers from contacting the shims so the applied pressure would not induce an unfavorable/uncontrolled strain state. A final layer of Kapton film and the top aluminum plate was placed on top, and the stack was transferred to the hot press, where the preload weights were attached to the tabbed fibers. The specimens were then forced air-cooled

to room temperature (-10°C/min). The preload weights, and then Kapton films were subsequently removed.

Weight selection was an important factor for designing these validation experiments. The different applied pre-loads had to induce a discernable strain shift (estimated by the model) to be quantified by the micro-Raman strain measurement technique [16] [17]. Additionally, the pre-load had to maintain a straight fiber through processing, which could induce fiber bending resin flow and/or buckling upon CTE contraction. In the end, 1g, 4g, and 8g weights maintained a straight fiber while providing a discernible change in the initial strain state.

FE MODEL TO PREDICT MICRO-COMPOSITE RESIDUAL STRESS

Accurate FE models of experiments are required to predict the residual stresses in micro-model composites. The simplest case of a model composite is a single fiber micro-composite, comprising of a single fiber embedded mid-plane in a matrix film. Carbon fiber has been modeled as a transversely isotropic elastic material with different CTE in the longitudinal and transverse direction as shown in Table 1.

Table 1. Material properties for AS4 carbon fiber [18] [19].

Elastic constants	E_{11} (GPa)	E_{22} (GPa)	ν_{12}	ν_{23}	G_{12} (GPa)	G_{23} (GPa)	α_{11} (μstrain/°C)	α_{22} (μstrain/°C)
AS4 Carbon fiber	235	14	0.2	0.25	2.8	5.6	-1.2	5.5

With the use of Raman spectroscopy, we can validate the residual stress predictive capability before moving on with more complex geometry, such as the pullout model, where resin thickness has significant variation around the meniscus. Further application of the predictive residual stress will be in the traction laws derived from pullout testing. However, the first step in generating accurate FE models is to incorporate the residual stresses induced from processing. Such residual stresses originate from the coefficient of thermal expansion (CTE) mismatch between constituents, in this case, the fiber and matrix. It is critical to accurately account for thermally induced residual stresses so that the appropriate applied strain matches in both the FE simulation and experiment. Figure 6 shows the FE model geometry for the single fiber micro-composite, these dimensions are representative of experimental specimens.

<u>The following experimental steps are modeled using the FE geometry and simulations:</u>

1. Applying preload (pre-defined weight) to the fiber at melt process temperature
2. With the preload, cooling the system down to room temperature (from the stress-free temperature to room temperature)
3. Removing the preload

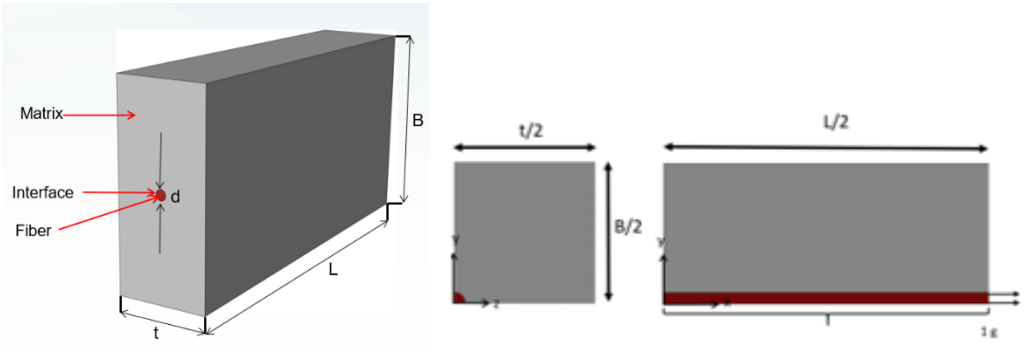

(a) (b)

Figure 6. FE model for single fiber fragmentation (t/d ≈ 14.5, L/d ≈ 285).

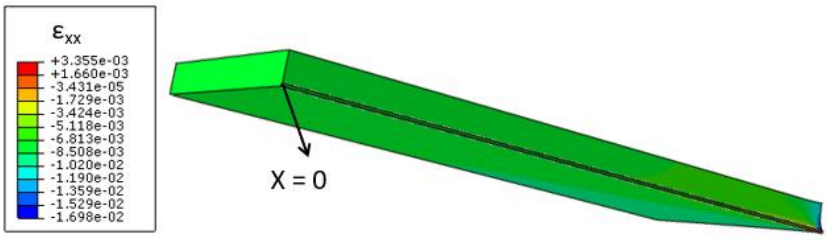

(a)

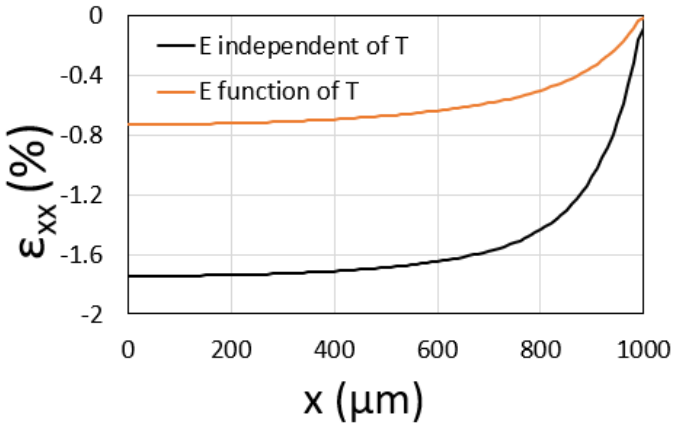

(b)

Figure 7. (a) ε_{xx} (residual axial strain) after removing preload of 1g (b) Residual axial strain considering E independent of T and E function of T

A quarter-symmetric micro-composite model has been generated for the analysis as shown in Figure 6. Mesh convergence studies have been done from a mesh size of 3 to 0.75µm. It has been determined that mesh is converged when mesh sizes were less than 2µm. Plane y = B/2 and z = t/2 are in the stress-free condition; a symmetric condition is applied to plane y = 0 and z = 0. Figure 7 shows the residual strain (axial strain) observed after removing preload of 1g. The end effects due to the shear-lag along the fiber are visible in Figure 7 (a). It's important to note that most of the literature assumes E independent T for measuring residual stress and over-predicts stresses and strains [20] [21]. Figure 7 (b) shows the residual axial strain considering E independent of T and E function of T. It is very clear that axial strain predicted by considering E function of T is almost half the value compared to the case where E is independent of T. Figure 8 shows ε_{xx} along the length of the fiber after removing preload

1g, 4g and 8g (Free fiber end at 1000µm). An increase in the preload will decrease the residual stress in the micro-composites. Practically it is difficult to achieve zero residual stress as the required preload is very close to the fiber breaking strength.

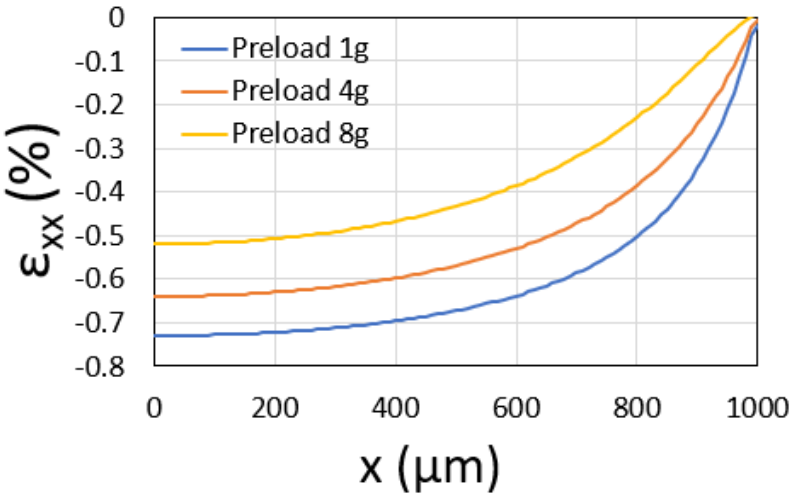

Figure 8. ε_{xx} along the length of the fiber after removing preload 1g, 4g, and 8g (Free fiber end at 1000µm).

The residual stress (strain) calculation for the single fiber specimens offers a refined mesh that can be implemented in short fiber array representative volume elements (RVEs) [22] [23]. Calculating the residual thermal stress is an important factor when replicating an experimental procedure. This builds upon the SFFT model and will be used to validate the simplest case of a single fiber micro-composite once cohesive traction separation laws are generated for the interface. After validation, the residual stress model can then be applied to model-fiber-array composites with added complexity.

RAMAN MEASUREMENT RESULTS

Using a Renishaw Qontor Raman microscope, a strain vs. Raman peak shift calibration curve was generated for AS4 fibers. Using the calibration curve, carbon fibers with different processing-applied preloads were observed in the matrix. A good metric for validation was comparing the bulk residual strain in the micro-composite with the FE model. This measurement was made in the center of the SFFT specimen, far away from the edges, where the strain would be constant. For the three pretension loads, 1g, 4g, and 8g, there was a good correlation between the FE model and the experimentally measured values (at most 5% mismatch), as shown in Figure 9. This is a good indication that the FE model and experimental inputs are mimicking the physical specimens we can produce experimentally.

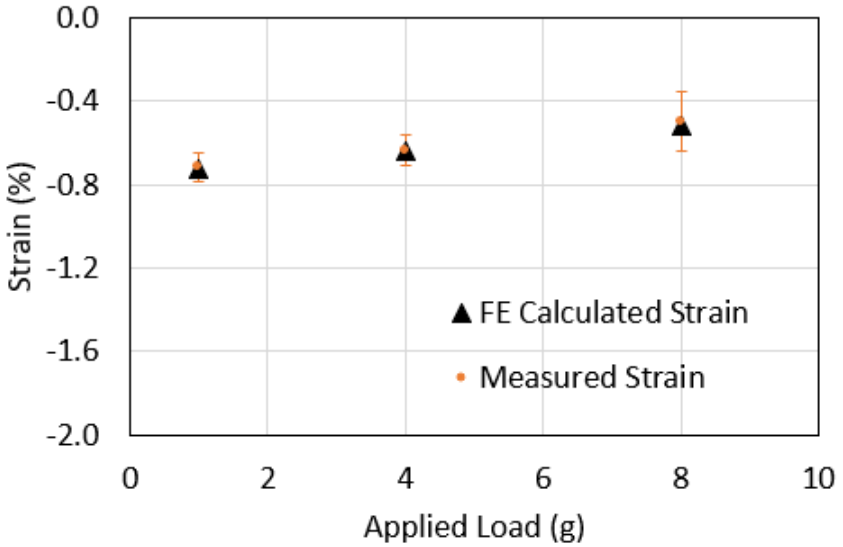

Figure 9. Bulk-level FE calculated residual strain for given preload conditions compared with experimentally measured values (1000µm from the edge).

CONCLUSION AND FUTURE WORK

The Raman strain measurement technique provides a good overall correlation with the FE model predicted residual stress. For the given thermal processing conditions (thermal loading) and mechanical loading, the predicted residual strains are on the right order of magnitude. The compressive loading, in this case, thermal & mechanical pre-loading, matches the simple analytical and developed FE models. A material agnostic computational model was developed with detailed experimental inputs to predict the thermal residual stress developed in the TPCs. Having validated a simple case with the FE model, we can apply it to more complicated geometries, such as the pullout test geometry where residual stress greatly influences the mechanical response.

ACKNOWLEDGEMENTS

This research was sponsored by ExxonMobil Research and Engineering Company, and National Aeronautics and Space Administration under Grant and Cooperative Agreement No. 80NSSC20M0164, issued through the Aeronautics Research Mission Directorate, Transformative Aeronautics Concepts Program, University Leadership Initiative.

REFERENCES

[1] Parlevliet PP, Bersee HEN, Beukers A. Residual stresses in thermoplastic composites—A study of the literature—Part I: Formation of residual stresses. Composites. Part A, Applied science and manufacturing 2006;37(11):1847-1857.

[2] Chapman TJ, Gillespie JW, Pipes RB, Manson J-E, Seferis JC. Prediction of Process-Induced Residual Stresses in Thermoplastic Composites. Journal of Composite Materials 1990;24(6):616-643.

[3] Parlevliet PP, Bersee HEN, Beukers A. Residual stresses in thermoplastic composites – a study of the literature. Part III: Effects of thermal residual stresses. Composites. Part A, Applied Science and Manufacturing 2007;38(6):1581-1596.

[4] Chen BR, Parambil NK, Deitzel JM, Gillespie JW, Vo LT, Sarosi P. Title: Interfacial Shear Strength (IFSS) and Absorbed Energy versus Temperature in Carbon Fiber-Thermoplastic Composites via Single Fiber Pullout Testing Authors (names are for example only). American Society for Composites 35th Technical Conference 2020:959-970.

[5] Chan TW, Isayev AI. Quiescent polymer crystallization: Modelling and measurements. Polymer engineering and science 1994;34(6):461-471.

[6] Nakamura K, Katayama K, Amano T. Some Aspects of Nonisothermal Crystallization of Polymers. 11. Consideration of the Isokinetic Condition. Journal of Applied Polymer Science 1973;17(4):1031-1041.

[7] Ding Z, Spruiell JE. Interpretation of the Nonisothermal Crystallization Kinetics of Polypropylene Using a Power Law Nucleation Rate Function. Journal of Polymer Science Part B: Polymer Physics 1997;35(7):1077-1093.

[8] Patel RM, Spruiell JE. Crystallization Kinetics During Polymer Processing -Analysis of Available Approaches for Process Modeling. Polymer Engineering and Science 1991;31(10):730-738.

[9] Mubarak Y, Harkin-Jones EMA, Martin PJ, Ahmad M. Modeling of non-isothermal crystallization kinetics of isotactic polypropylene. Polymer (Guilford) 2001;42(7):3171-3182.

[10] Hammami A, Spruiell JE. Quiescent Nonisothermal Crystallization Kinetics of lsotactic Polypropylenes. Polymer Engineering and Science 1995;35(10):797-804.

[11] Eduljee RF, Gillespie JW, Mccullough RL. Residual stress development in neat poly (etheretherketone). Polymer Engineering and Science 1994;34(6):500-506.

[12] Eduljee RF, Gillespie JW, Mccullough RL. On the application of micromechanics to the prediction of macroscopic thermal residual stresses in short-fiber reinforced polyetheretherketone. Polymer Engineering and Science 1991;31(17):1257-1263.

[13] Lawrence WE, Seferis JC, Gillespie Jr JW. Material response of a semicrystalline thermoplastic polymer and composite in relation to process cooling history. Polymer Composites 1992;13(2):86-96.

[14] Chapman TJ, Gillespie JW, Pipes RB, Manson J-E, Seferis JC. Prediction of Process-Induced Residual Stresses in Thermoplastic Composites. Journal of Composite Materials 1990;24(6):616-643.

[15] Gillespie JW, Chapman TJ. The Influence of Residual Stresses on Mode I Interlaminar Fracture of Thermoplastic Composites. Journal of Thermoplastic Composite Materials 1993;6(2):160-174.

[16] Huang Y, Young RJ. Effect of fibre microstructure upon the modulus of PAN- and pitch-based carbon fibres. Carbon (New York) 1995;33(2):97-107.

[17] Qian X, Wang X, Zhong J, Zhi J, Heng F, Zhang Y, Song S. Effect of fiber microstructure studied by Raman spectroscopy upon the mechanical properties of carbon fibers. Journal of Raman spectroscopy 2019;50(5):665-673.

[18] Parambil NK, Gururaja S. Bridging micro-to-macro scale damage in UD-FRP laminates under tensile loading. International Journal of Mechanical Sciences 2019;157-158:184-197.

[19] Trinquecoste M, Carlier JL, Derré A, Delhaès P, Chadeyron P. High temperature thermal and mechanical properties of high tensile carbon single filaments. Carbon (New York) 1996;34(7):923-929.

[20] Nairn JA. Analytical Fracture Mechanics Analysis of the Pull-Out Test Including the Effects of Friction and Thermal Stresses. Advanced Composites Letters 2000;9(6):373-383.

[21] Zhandarov S, Mäder E. Analysis of a pull-out test with real specimen geometry. Part II: the effect of meniscus. Journal of Adhesion Science and Technology 2013;28(1).

[22] Parambil NK, Gururaja S. Micromechanical damage analysis in laminated composites with randomly distributed fibers. Journal of composite materials 2016;50(21):2911-2924.

[23] Parambil NK, Gururaja S. Micro-scale progressive damage development in polymer composites under longitudinal loading. Mechanics of Materials 2017;111(1):21-34.